Evidence for unbenignant nature of glucose as a replacement for water in purple membrane

Nicholas J. Gibson* and Joseph Y. Cassim‡

*Department of Chemistry, University of Arizona, Tucson, Arizona 85721; and ‡Department of Microbiology and Program in Biophysics, College of Biological Sciences, The Ohio State University, Columbus, Ohio 43210 USA

ABSTRACT The net angle (θ_α) between the seven helical segments of the bacteriorhodopsin (bR) polypeptide and the normal to the membrane plane of the purple membrane (PM) is ~0° when determined by oriented far-ultraviolet (UV) circular dichroism (OCD) and midinfrared linear dichroism (IRLD). However, θ_α is ~11° when determined by high-resolution electron cryo-microscopy and electron diffraction (EMD). The spectral studies are made with fresh hydrated PM films at ambient temperature, whereas diffraction studies are made with aged glucose-embedded PM at −120 to −268°. The current study presents oriented far-UV OCD results of hydrated PM films embedded with glucose, which can best be interpreted as a change in the magnitude of θ_α ($\Delta\theta_\alpha$) from 0 to 23° as a consequence of glucose embedment. Possible alternative explanations contrary to this conclusion are discussed and ruled out. Therefore, it is suggested that a θ_α of ~11° as determined by the EMD method may not be an intrinsic structural characteristic of the native PM but an induced one. The differences in the $\Delta\theta_\alpha$ value due to glucose embedment as determined by the two different approaches (23 vs. 11°) may be attributed to the drastic differences in the experimental conditions used, especially temperature. It is expected that at extremely low temperatures protein dynamics would be highly restricted and $\Delta\theta_\alpha$ relatively curtailed. It is concluded that glucose may not be as benign to biological structures as has been assumed in the past.

INTRODUCTION

The retinylidene protein bacteriorhodopsin (bR), the sole protein component of the purple membrane (PM) of *Halobacterium halobium,* is presently the best-characterized example of a membrane protein and is considered by many to be the paradigm of transmembrane transport proteins (for comprehensive reviews, see references 1–8 and references cited therein). This protein is composed of a single, 26,866-D, 80% α-helical/20% aperiodic, polypeptide chain of 248 amino acids. It comprises 75% of the PM dry weight, with the remainder being lipids. The polypeptide chain is enfolded seven times into the PM bilayer, embedding ~80% of the amino acids within the hydrophobic environment of the membrane. Although the bilayer-spanning polypeptide segments are predominantly α-helical in secondary structure, there is strong evidence that they are not solely of the classical α_I-type–like helix. Theoretically, according to the Ramachandran plot, right-handed α-helices can exist as structural types ranging from the pure α_I (dihedral angles, ϕ 127° and ψ 128°) to the α_{II} (dihedral angles, ϕ 87° and ψ 162°) (9). In the α_I-type, according to molecular modeling, the planes of the amide groups are oriented within the range of 0 to 10° with respect to the helix axis. However, in the α_{II}-type, they are significantly tilted away from the helix axis. (*a*) The anomalous blue-shifted position of the amide I band of the bR and the anomalous large splitting of the parallel and perpendicular modes of this band observed in the mid-infrared (IR) spectrum suggest significant α_{II}-type–like characteristics present in the helix of the bR (10). (*b*) The Raman spectroscopic analysis of the bR in the PM has been shown to be consistent with only half of the bR helices having α_I-type characteristics (11). (*c*) The magnitude of the ellipticities of the far-ultraviolet (UV) solution circular dichroic (CD) spectrum of the PM at every wavelength have been shown to be two thirds of that of myoglobin. Since the secondary structures of myoglobin and bR are similar except that the α-helix of myoglobin is very nearly exclusively of the α_I-type, this would be theoretically expected if the helices of the bR consist on the average of approximately nearly equal amounts of α_I and α_{II} type characteristics (12). (*d*) According to the electronic theories of amides, the protein $n - \pi^*$ transitions in the far-UV are polarized along the C=O bonds of the amide groups of the protein (13). The amide groups are expected to be aligned with the helix axis within the range 0 to 10° in the α_I-type and, therefore, for incident light propagated down the helix axis (as is the case in oriented film studies) the contribution of this transition to the CD should be reduced by ~80–75% of the value for light propagated randomly (as is the case in solution studies) (14, 15). Experimentally, a reduction of ~50% has been observed for polypeptides and proteins with almost solely α_I-type characteristics (15, 16). In the case of the bR, this reduction was limited to only ~15%. This provides strong support for the hypothesis that the planes of the amide groups in the bR are tilted an appreciable amount away from the helix axis, since the planes of the amide groups in an α_{II}-type helix are expected to be tilted within the range of 35 to 45° with respect to the helix axis based on molecular models (12, 17). (*e*) The net segmented tilt angle θ_α (the average angle between the seven transmembrane polypeptide segments of the bR and the membrane normal of the PM)

Address correspondence to J. Y. Cassim.

0006-3495/93/05/1434/11 $2.00

determined for the native state of the bR by the analysis of the far-UV oriented circular dichroism (OCD) of the PM (for a detailed discussion of this method, see the following section) has been shown to be consistent with the one determined by an independent analytical spectral method, mid-infrared linear dichroism (IRLD), only when it is assumed in the IRLD analysis that the characteristics of the α-helices of the bR consist, on the average, of 60% α_I and 40% α_{II}. The change in the magnitude of the net angle ($\Delta\theta_\alpha$) resulting from the transformation of the bR from the native to the bleached state has also been shown to be consistent when determined by these two independent methods, but only if based on the same assumption of the nature of the bR helices (17–19).

θ_α has been shown to be most likely 0° in hydrated PM films by OCD and IRLD analyses as discussed above (17, 19, 20). That is, the helical segments of the native bR must all be oriented nearly parallel to the PM normal. An identical orientation has been reported for the helical segments of the alamethicin protein embedded in well-oriented multilamellar films of dilauroylphosphatidylcholine (DPhPC) (16, 21). On the other hand, IRLD analyses of the bR in hydrated and air-dried PM films have repeatedly estimated the θ_α value of the native form of bR to be ~24–29° based on the assumption that the characteristics of the α-helices of the bR are solely α_I (22–26). In addition, when the bR is light bleached in the presence of hydroxylamine, the resulting $\Delta\theta_\alpha$ is 24° if determined by the OCD method (18). However, if $\Delta\theta_\alpha$ is determined by the IRLD method for this perturbation, $\Delta\theta_\alpha$ is 47° when the characteristics of the helices are assumed to be, on the average, solely α_I (23). But if the characteristics are assumed to be ~60% α_I and 40% α_{II}, then this $\Delta\theta_\alpha$ becomes 24° (17, 18). Paradoxically, the emerging model for the structure of the bR based on the high-resolution electron microscopy and electron diffraction (EMD) studies of the PM by Henderson and co-workers (1, 8, 27–31) for over a decade and a half has repeatedly suggested that the helical segments of the bR are distinctively on the average tilted, albeit of a relatively small angle, with respect to the membrane normal. In Fig. 15 of their recent publication (8), three of the seven transmembrane segments of the bR molecule are shown to be relatively straight but tilted at various degrees from the membrane normal, while the remaining ones are shown to be slightly kinked and bent, also resulting in deviations of segmental parallelism with the membrane normal. However, as shown, the segmental tilting does not seem to eliminate much of the relative intersegmental parallelism. On the basis of the data presented in their Fig. 15, θ_α can be estimated to be ~11°, a value that was previously reported by Nabedryk and Breton (32) citing Henderson as the source. It should be realized that while the OCD and IRLD studies are mostly made with hydrated films of freshly prepared PM specimens at ambient temperature, in contrast, EMD studies are made with aged octylglucoside treated and glucose-embedded PM specimens subjected to very high vacuum at −120 to −268°C under relatively high energy radiation. To add to this paradox, x-ray investigations of the in-plane projected structure of the bR in dry and wet PM pellets at ambient temperature have provided evidence seemingly in support of the EMD analyses (1, 33). Further inconsistencies between EMD and OCD results became apparent when the transition from the ground state, bR_{568}, to the excited photointermediate state, M_{412}, of the bR was studied by the two methods. The OCD method detected a reversible $\Delta\theta_\alpha$ of 10 ± 5° as a result of this transition in hydrated PM films at −70°C (34). In contrast, the EMD method failed to detect any significant observable change in the structure of the bR (29). Initial Fourier transform IR difference spectral studies also failed to detect any significant changes, even though studies were made with glucose-free hydrated films of PM (35–37). However, more recent studies of this kind have been able to detect changes, even those involving the bR backbone (38, 39). In addition, neutron and x-ray diffraction analyses of the structural consequences of this transition have revealed changes in the tilt of bR helical segments (40–42). Although these changes are somewhat less dynamic than the ones suggested by the OCD study, most likely because of differences in experiment conditions used, nevertheless, they are in contradiction to the static results of the EMD study of glucose-embedded PM specimens.

The goal of the present OCD study of the PM is to attempt to find a logical explanation for all these apparently conflicting findings regarding the structure of the native bR in the PM and its photo-induced conformational dynamics. The stated purpose for the use of glucose in EMD studies of the PM is to prevent in vacuo structural destruction of the membrane (27, 28). It has generally been assumed that sugars such as glucose are benign replacements for liquid water in membranes, although there is no solid evidence to support such an assumption (1, 8, 27, 28, 30, 31, 43–46). In a previous study using the OCD method, it was observed that exhaustive vacuum evacuation of the hydrated PM film at ambient temperature results in a $\Delta\theta_\alpha$ of ~21° (47). A very similar value, 19°, was found when the PM film was impregnated with dry glycerol (47). In addition, it was observed that the helical segments of alamethicin in DPhPC multilayers will also change their orientations in a similar manner when the degree of hydration is reduced (21). However, when the film was both impregnated with glycerol and exhaustive high-vacuum evacuated, the $\Delta\theta_\alpha$ remains within an experimental uncertainty of ±2° the same, that is 22°, indicating that a combination of the two perturbations does not result in any further change in the $\Delta\theta_\alpha$ value induced solely by either one. In this study it is shown that when the PM film is embedded with glucose the resulting $\Delta\theta_\alpha$ is 23° and, in addition, if the glucose effect is combined with

the dehydration one, the induced $\Delta\theta_\alpha$ remains 23°. Ironically, the glucose effect on θ_α is the same as that of dehydration. Clearly, instead of protecting the membrane against all the destructive effects of dehydration, glucose causes similar changes in the orientation of the helical segment of the bR. Logically, if glucose embedding causes a tilt of the bR segments in the PM films, it follows that it may also cause a similar effect on glucose-embedded PM specimens in EMD studies. This would suggest that the tilt of segments determined by EMD analyses may be an induced characteristic of the PM and not a native one. The differences in the magnitudes of the induced glucose effects in the two cases can probably be attributed to the differences in experimental conditions imposed on the PM, especially temperature. Arguments are presented to show how these findings of the glucose effect can bring about a consolidation of the many conflicting findings of the past regarding the structure and photo-induced structural dynamics of the bR in the PM. Furthermore, these findings clearly suggest that glucose may not be as benign to biological structures as has been assumed in the past.

MATERIALS AND METHODS

PM preparation

PM was isolated from the S9 strain of *Halobacterium salinarium* (formerly *halobium*) by the method of Becher and Cassim (48) with the omission of the sucrose gradient step. However, many washing steps were incorporated into the purification process. Although this modified procedure reduced the PM yield, it produced preparations of equal or greater purity without exposing the PM to sucrose (49). Centrifugations were accomplished at the relatively low speed of 22,000 *g* for 90 to 120 min in order to produce preparations uncontaminated by red membrane.

Film preparation

The PM specimens were suspended in double-distilled water to an OD_{568} of 0.2 and 0.3 for films for far-UV spectral studies and 2.5 to 3.0 for films for visible and near-UV spectral studies. The solutions were filtered using Gelman model GA-1 5-μm filters (Gelman Sciences, Inc., Ann Arbor, MI) and degassed by stirring under an aspirator. Approximately 0.75 ml of a given solution was then layered on a 25-mm-diam quartz optical flat (suprasil-S Precision Cells, Inc., Hicksville, NY) and allowed to dry in a desiccator containing Drierite or a saturated $LiCl_2$ solution (20% relative humidity environment). The PM films were incubated for 24 h in a desiccator containing a saturated K_2SO_4 solution (95% relative humidity environment). The average film used for far-UV spectral studies had an OD_{193} of 0.34 and an OD_{568} of 0.008, indicating these films to be ~6–12 monolayers thick, based on an OD_{568} of 0.0.0016 for a PM bilayer (50).

Quality control of these films has been previously discussed in detail (18). Films were monitored for the presence of mosaic spread by several methods. A drop of sample, similar to the ones used for film preparation, was examined by electron microscopy to be sure the membranes were not aggregated and were drying parallel to the film surface. Also the visible linear dichroism of the films was determined. Native hydrated PM films exhibited retinylidene out-of-plane angles of 21.2 ± 2°. This value is in excellent agreement with the one published by Heyn et al. (51), who used neutron diffraction technique to demonstrate that mosaic spread was negligible in their PM films. Therefore, it is a reasonable conclusion that the films used in the present study must be similar to theirs as far as mosaic spread is concerned. Finally, a further check for mosaic spread was conducted by gradually forming a PM film sufficiently thick to allow critical investigation of the visible circular dichroism (CD) fine spectrum. The finding of no evidence of the characteristic biphasic CD band of PM suspensions suggested the absence of any appreciable tilt of the membrane disks with respect to the measuring light (20).

These films were than embedded with glucose (certified A.C.S. anhydrous dextrose [D glucose], Fisher Scientific Co., Fair Lawn, NJ) by overlaying them with sufficient glucose solution to cover the entire film. Glucose concentrations used varied from 0.5 to 0.05%. The films were finally redried in the desiccator as indicated above.

Spectroscopy

Absorption spectra were recorded on a spectrophotometer with a far-UV modification and a scattered transmission accessory (Cary 118C; Varian Associates Inc., Palo Alto, CA). CD spectra were recorded on a spectropolarimeter with a CD attachment (Cary 60 and 6003, respectively; Varian Associates Inc. or model J-500A; Jasco Inc., Easton, MD). Experimental procedures were as previously described (20).

OCD method for determining θ_α between seven transmembrane polypeptide segments of bR and PM normal

The far-UV electronic spectra of helical proteins have been assigned to the very weak $n - \pi^*$ transitions and the strong $\pi - \pi^*$ (NV_1) transitions of the polypeptide amide groups (for a recent review of the theories of the CD of proteins see Woody [52] and references therein). According to the quantum mechanical interpretation of α-helical protein spectra, the degenerate $n - \pi^*$ transitions give rise to a negative approximately Gaussian CD band, which is polarized somewhat perpendicular to the helix axis of the protein and centered at ~224 nm. The degenerate $\pi - \pi^*$ (NV_1) transitions undergo strong exciton coupling because of the one-dimensional crystalline structure of the helical protein and split into three mutually orthogonal transitions. One resulting transition dipole moment is polarized parallel to the helix axis and gives rise to a negative Gaussian CD band centered at ~207 nm. The other two, which are double degenerate, are polarized perpendicular to the helix axis. They give rise to a positive Gaussian CD band centered at ~190 nm and a pair of CD bands with the biphasic shape of the derivative of a Gaussian band centered near 190 nm with the positive lobe on the long wavelength side.

The OCD method for determining θ_α in the PM is based on the change of the rotational strength of the 207-nm CD band as the angle between the directions of the protein helix axis and the incident light are varied. If R_o is the rotational strength of the 207-nm band when the helix axis and the incident light are randomly oriented to each other, then $R_o = (2R_\perp + R_\parallel)/3$ because of the cylindrical symmetry of the α-helix. $R_\perp$ and $R_\parallel$ are the rotational strengths of CD bands due to transition dipole moments polarized perpendicular and parallel to the helix axis, respectively. However, since the 207-nm band is polarized along the helix axis, then $R_\parallel = 0$ and therefore, $R_o = \frac{2}{3}R_\perp$. The rotational strength of 207-nm band, R_α, at any angle θ_α is given by $R_\alpha = R_\perp \sin^2\theta_\alpha + R_\parallel \cos^2\theta_\alpha$. Therefore, for the 207-nm band R_α becomes $R_\alpha = R_\perp \sin^2\theta_\alpha = \frac{3}{2}R_o \sin^2\theta_\alpha$ and finally, $\sin^2\theta_\alpha = \frac{2}{3}(R_\alpha/R_o)$ or $\theta_\alpha = \sin^{-1}[\frac{2}{3}(R_\alpha/R_o)]^{1/2}$. Clearly, if $R_\alpha = R_o$ then $\theta_\alpha = 54.736°$. This is the theoretically expected value for θ_α in the case of complete randomization of the helix axes orientations with respect to the incident light direction. In ethanol-treated PM films, the helical segments of the bR are conformationally identical to those in the native state in regards to secondary structure. However, they are completely randomly oriented in respect to the membrane normal. The unequivocal proof for this comes from IRLD spectral analysis, which indicates a value of 54.735° ± 0.001° for the θ_α of bR in ethanol-treated PM films (17).

The OCD spectra of hydrated native PM films are free of any observable contributions from the 207-nm band (20). This, according to theory, is indicative of all the helical segments of the bR being oriented nearly parallel to the PM normal. That is, θ_α is most likely 0° for the native PM. This was confirmed independently by IRLD analysis (17). Therefore, $\Delta\theta_\alpha$ can be determined for any perturbation of the PM from the equation derived above for θ_α by obtaining R_α from the difference (ΔOCD) spectrum between the perturbed and the native PM OCD spectra and R_0 from the ΔOCD spectrum between the ethanol-treated and the native PM OCD spectra. A number of $\Delta\theta_\alpha$ values determined by this method for a variety of perturbations of the PM have been confirmed independently by the IRLD method (17, 18). In addition, it is apparent from this equation for θ_α that the amplitude of the 207-nm band must be linearly proportional to $\sin^2\theta_\alpha$. This was recently experimentally verified by studying the OCD of the 20-amino acid peptide alamethicin embedded in DPhPC multibilayer films, which could be tilted by fixed angles with the incident light (16).

RESULTS AND DISCUSSION

Far-UV OCD spectra

The far-UV OCD spectrum of a hydrated PM film before (*curve 1*) and after (*curve 2*) embedding with 0.05% glucose as recorded on the Cary spectropolarimeter is shown in Fig. 1 *A*. The OCD spectrum of ethanol-treated PM (*curve 3*) is also shown in the same figure. The ΔOCD spectra between the two modified films and the native one are shown in Fig. 1 *B*. In both cases, the ΔOCD spectra results in nearly Gaussian bands centered at ~207 nm with the amplitude of the ethanol-induced one (*curve 2*) being ~4.3 times greater than that of the glucose-induced one (*curve 1*). On the basis of the previously derived equation for θ_α (see Materials and Methods), $\Delta\theta_\alpha$ is 23° because of embedding in 0.05% glucose. However, spectra recorded with film embedded with higher concentrations of glucose exhibited spectra significantly different than the one shown in Fig. 1 *A*. This effect was greater in spectra recorded with the Jasco spectropolarimeter than with the Cary instrument because of the inherent differences in the far-UV optical characteristics of the two instruments. The spectrum of a PM film embedded with 0.25% glucose is shown in Fig. 2 *A*. Comparing this spectrum with that of 0.05% glucose embedment in Fig. 1 *A*, it is apparent that the 207-nm band and especially the positive 197-nm band have undergone dramatic changes not present in the spectrum in Fig. 1 *A*. These changes can be attributed to the increased glucose concentration, which increases the absorbance of the film. This increase in absorbance combined with the particulate characteristics of the PM can result in optical distortion of the CD spectrum, such as absorption flattening (53). Absorption flattening effects would be most pronounced at the absorption maximum of the PM film, which is centered at ~193 nm. The extent of this optical distortion in the OCD spectrum can be determined and corrected for by use of the ΔOCD spectrum of glucose-embedded PM treated with ethanol minus that of native PM treated with ethanol. This is shown in Fig. 2 *B* (*curve 2*). The rationale for this is the fact that ethanol treatment completely randomizes the helical segments in respect to the membrane normal and, therefore, any glucose-induced differences cannot be due to changes in θ_α but must be due to optical distortions. Also, the peak amplitude of the ethanol-treated PM ΔOCD curve (*curve 2* in Fig. 2 *B*) is clearly at the absorption maximum of the PM film. If the same study is made with 0.05% glucose, the OCD of the ethanol-treated glucose-embedded film is identical to that of the ethanol-treated native film. This provides evidence that the 0.05% glucose-embedded PM OCD spectrum is probably essentially free of any optical distortions. In Fig. 2 *B* it is obvious that ΔOCD spectrum of the 0.25% glucose-embedded PM film minus that of the native PM film (*curve 1*) is not a nearly Gaussian band centered at ~207 nm, as in the case of the 0.05% glucose embedment (*curve 1*) in

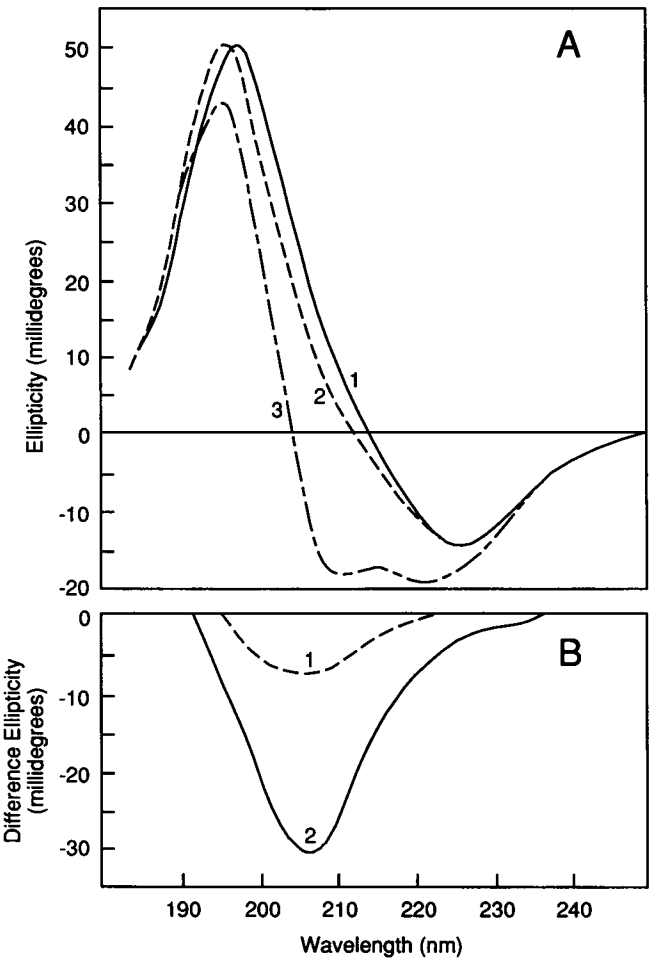

FIGURE 1 The film far-UV OCD (glucose-embedment concentration 0.05%). (*A*) Spectra of (*1*) native, (*2*) glucose-embedded, and (*3*) ethanol-treated PM. (*B*) Difference spectra of (*1*) glucose-embedded minus native and (*2*) ethanol-treated minus native PM. The angle θ_α for the ethanol-treated PM film has been shown to be 54.74° from IRLD spectral analysis, which establishes this film as an ideal random state standard. $\Delta\theta_\alpha$ resulting from glucose embedment, calculated from the equation $\theta_\alpha = \sin^{-1}[\frac{2}{3}(R_\alpha/R_0)]^{1/2}$ with R_α and R_0 obtained from *curves 1* and *2* in *B*, respectively, is 23°. See text for details.

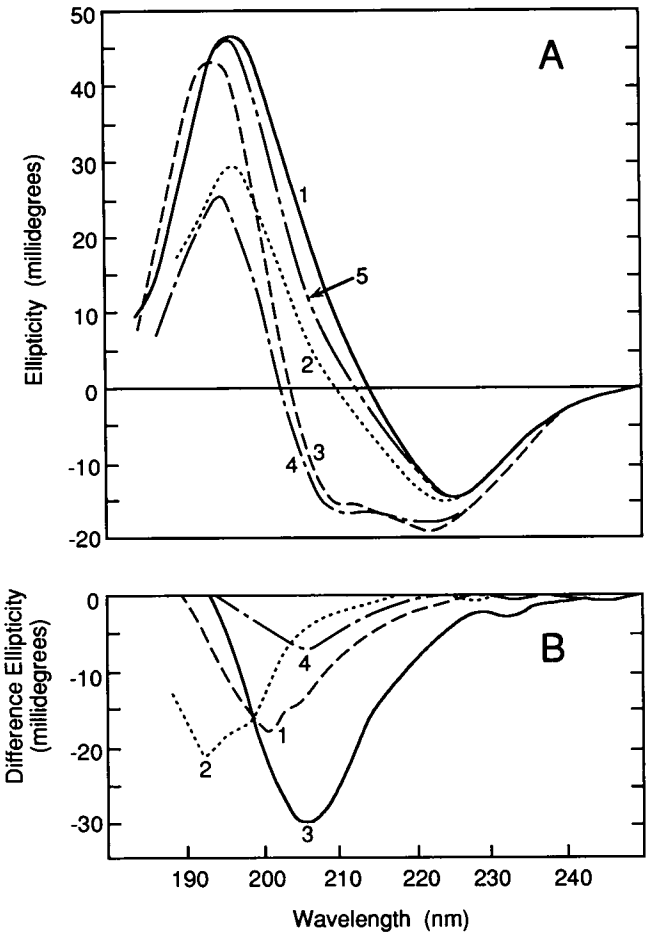

FIGURE 2 The film far-UV OCD (glucose-embedment concentration 0.25%). (*A*) Spectra of (*1*) native, (*2*) glucose-embedded, (*3*) ethanol-treated, (*4*) glucose-embedded ethanol-treated, and (*5*) corrected glucose embedded PM. (*B*) Difference spectra of (*1*) glucose-embedded minus native, (*2*) glucose-embedded ethanol-treated minus ethanol-treated, (*3*) ethanol-treated minus native, and (*4*) corrected glucose-embedded minus native PM. The corrected glucose-embedded curve is the absolute sum of *curve 2* in *A* and *curve 2* in *B*. $\Delta\theta_\alpha$ resulting from glucose embedment, calculated from the equation $\theta_\alpha = \sin^{-1}[\frac{2}{3}(R_\alpha/R_0)]^{1/2}$ with R_α and R_0 obtained from *curves 4* and *3* in *B*, respectively, is 23°. See text for details.

Fig. 1 *B*, but a distorted band centered at ~200 nm. However, if the absolute magnitude of the ΔOCD curve of the ethanol-treated 0.25% glucose-embedded and ethanol-treated native PM films (*curve 2* in Fig. 2 *B*) is added to the OCD curve of the 0.25% glucose-embedded PM film (*curve 2* in Fig. 2 *A*), the corrected resultant curve (*curve 5* in Fig. 2 *A*) becomes very similar to that of the 0.05% glucose-embedded OCD curve (*curve 2* in Fig. 1 *A*). The ΔOCD curve of the corrected resultant curve minus that of the native PM one (*curve 4* in Fig. 2 *B*) is clearly a nearly Gaussian band centered at ~207 nm with an amplitude ~ 1/4.2 times that of the ethanol-treated ΔOCD band. The resulting $\Delta\theta_\alpha$ is also ~23°. The fact that this value of $\Delta\theta_\alpha$ is in excellent agreement with the one for 0.05% glucose embedment indicates that the experimentally induced optical distortion effects have been successfully removed from the spectrum of the 0.25% glucose-embedded PM film. Also, it has been observed that, if glucose-embedded films are subjected to exhaustive high-vacuum evacuation, the $\Delta\theta_\alpha$ remains unchanged from the 23° value.

Theoretically, a $\Delta\theta_\alpha$ signifies a change in the average angle between the helix axes and incident light directions. In the OCD studies of PM films, the incident light is oriented parallel to the film normal. Therefore, this change could be due to a change in the angle between the helix and the membrane normal of the PM resulting from a structural change of the bR in the PM. However, it could also be due to a change in the angle between the membrane and film normals, resulting from a change in the mosaic spread angle (θ_m) of the PM discs in the film. Since the PM films used for OCD studies are very thin, consisting of no more than 6–12 monolayers, θ_m is estimated to be nearly zero for the native PM film (see Materials and Methods). Therefore, in OCD studies the incident light is essentially directed perpendicular to the membrane plane. If one assumes $\Delta\theta_m$ to be the underlying cause for $\Delta\theta_\alpha$, then one must conclude that the perturbing agents used must be altering the physical ordering of the PM discs in the film. It is difficult to see how this could be possible, since the close-packed nature of the PM film would not allow for any major three-dimensional reordering without a large input of energy to overcome the electrostatic interactions between the PM discs. In past studies of the OCD of perturbed PM films, the $\Delta\theta_m$ explanation for the observed $\Delta\theta_\alpha$ was dismissed as a serious alternative possibility based on the following experimental observations (17, 18, 47, 49, 54). (*a*) The OCD changes are independent of film thickness. (If $\Delta\theta_m$ is the cause of $\Delta\theta_\alpha$, one would expect OCD changes to be sensitive to film thickness.) (*b*) Whether PM is bleached in suspension or in situ in film, the resulting OCD changes are the same. (*c*) When the PM film is layered with an overlying buffer solution, no changes are apparent, even after several days. (*d*) When the PM film is layered with a hydroxylamine solution in the dark, there are no OCD changes until the film is irradiated with intense light. (*e*) When the PM film is impregnated with glycerol, there are no OCD changes until the film is exposed to dry-nitrogen flushing, and this change is very rapidly reversed when the film is reexposed to ambient humidity (average 50% relative humidity). (*f*) The sodium-borohydride–reduced PM film has an OCD spectrum identical to the native PM one, with the OCD changes appearing only when the reduced film is irradiated with intense white light for a time. (*g*) When the exhaustively high-vacuum dehydrated PM film is reexposed to ambient humidity, the induced OCD change is very rapidly reversed. Similarly, in the present case, when glucose solution is layered on the PM film, the glucose solution forms a thick syrup, which becomes glasslike with further drying. However, the OCD changes

do not appear until the dried films are allowed to incubate in a 90% relative humidity environment for some time. It is clear that liquids layered onto PM films do not disturb the θ_α of PM films, as would be expected if $\Delta\theta_\alpha$ is the result of $\Delta\theta_m$. On the other hand, $\Delta\theta_\alpha$ seems to result from light radiation and critical and rapid removal and addition of water molecules. It does not seem possible that these agents can reorder the three-dimensional packing of the PM discs in the PM in such a manner as to cause a $\Delta\theta_m$ of 23°.

In view of the above evidence, it is most probable that the $\Delta\theta_\alpha$ of 23° resulting from the glucose embedding of the PM film is an inherent property of the PM and cannot be easily dismissed as an experimentally induced artifact such as optical distortions or three-dimensional structural reordering of the film. It is noteworthy that a similar $\Delta\theta_\alpha$ value ($22 \pm 2°$) has been observed as a consequence of a number of other perturbations of the native PM at ambient temperature, such as light bleaching in the presence of hydroxylamine, exhaustive high-vacuum dehydration, and dry-glycerol impregnation (17, 18, 47, 55). Importantly, $\Delta\theta_\alpha$ is completely reversible in all these cases. The ΔOCD spectra indicate that the glucose effect results essentially in the emergence of a 207-nm CD band, which results in a $\Delta\theta_\alpha$. This is predicted by the strong-coupling exciton theory of the optical properties of oriented helical polypeptides as a consequence of the helix axis and the incident light directions diverging from co-parallelism (14). Recently this prediction has received experimental verification (12, 16, 56). In fact, $\Delta\theta_\alpha$ was the explanation given previously to account for a similar 207-nm band emergence due to the bleaching of the native and chemically altered PM films in the presence of hydroxylamine (18). This explanation could be verified by another independent method, IRLD spectral analysis (17). However, the need for relatively very thick PM films for this kind of spectral analysis makes it technically formidable at present to use this method for glucose-embedded film studies.

An unambiguous interpretation of $\Delta\theta_\alpha$ in terms of molecular structure changes is difficult to make. A $\Delta\theta_\alpha$ of 23° signifies a change in the orientation of two or more helical segments of the bR with respect to the PM normal. This can be accomplished by two modes of protein structural dynamics: (*a*) molecular tumbling, in which there is a rotation of the protein molecule about an axis in the membrane plane, thus maintaining the relative orientations of the segments to each other; or (*b*) change in the tertiary structure of the protein, in which the relative orientation of the segments to each other are altered by tilting. However, molecular tumbling can be ruled out in the case of glucose embedding since diffraction analyses have demonstrated the retention of the crystalline order of the PM subjected to this perturbation (1, 8, 33).

Recently, it has been suggested that the changes in the dihedral angles of the protein helix may possibly account for the emergence of the 207-nm band in OCD studies (57). However, changes in dihedral angles are expected to have a very minor effect on the 207-nm band since this band is due to an excitonic transition that depends mainly on the orientation of the helix axis in respect to the incident light. On the other hand, such changes are expected to have much stronger effects on the 225- and 197-nm bands. It is apparent from Fig. 1 *A* there are no significant changes in these bands because of glucose embedding. This lack of significant changes in these bands also rules out any changes in the secondary structure of the bR because of this perturbation. It is apparent that the only explanation for the emergence of the 207-nm band as a result of glucose embedment, which has a sound theoretical basis and is consistent with all the experimental data, is that this perturbation causes tertiary structure changes in the bR as a result of the protein being tilted away from the PM normal.

Near-UV OCD spectra

The solution and film near-UV CD spectra of PM have revealed dramatic differences between the native and light-bleached states of the bR (18, 20). The near-UV CD can serve as a probe for changes in the orientations, interaction, and environments of the aromatic amino acid residues of the bR, notably phenylalanines, which have been shown to be located primarily around the inner hydrophobic core of the protein (18, 20, 58). A $\Delta\theta_\alpha$ of 24° coupled to a dramatic change in the near-UV CD of the light-bleached bR has been interpreted as resulting from a tertiary structural change of the bR, which opens up the protein and exposes its hydrophobic inner core to an aqueous environment (18, 20). This interpretation has been supported by the reduction in the frequencies of the amide transitions in the mid-IR range of the PM as a result of this perturbation (17). Similar near-UV spectral changes were noted during the formation of the M_{412} photointermediate state of the bR, except that the magnitude of the resulting $\Delta\theta_\alpha$ was reduced to $10 \pm 5°$, possibly because of the low temperature used to trap this transitory photostate (34).

The comparative near-UV OCD spectra of native, glucose-embedded, and exhaustive-vacuum dehydrated PM films are shown in Fig. 3. However, unfortunately, OCD film spectra are not always as sensitive to such changes as solution CD spectra, and glucose-embedding studies are not possible in solution. The dehydrated PM film spectrum is identical to the one previously published and is given here for comparison (47). It is apparent that glucose embedment has relatively minor effect on the near-UV OCD film spectrum of the PM. This is also true for vacuum dehydration and for dry-glycerol impregnation of PM films previously given (47). This indicates that the native anisotropism of the bR structure with respect to the average orientations of the aromatic rings of certain amino acid residues to the membrane plane is not lost because of these perturbations of

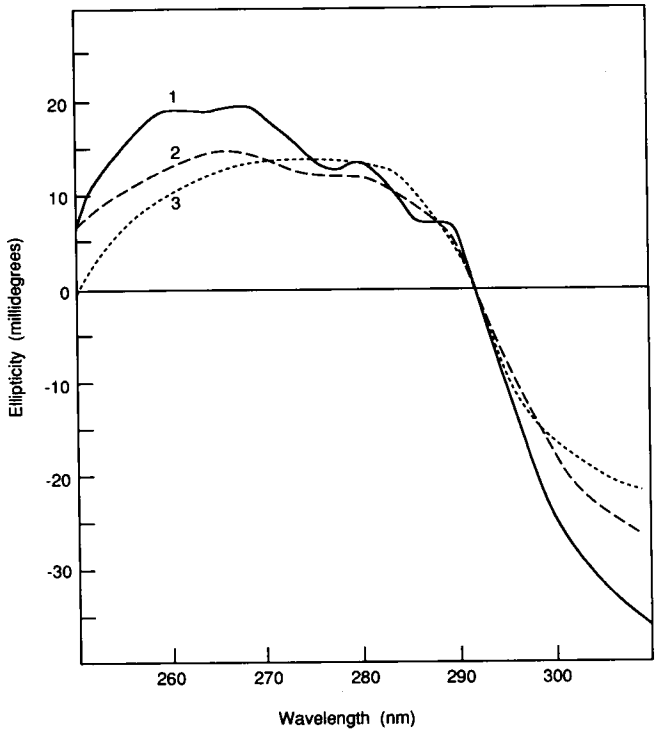

FIGURE 3 The film near-UV OCD spectra of (*1*) native, (*2*) glucose-embedded, and (*3*) exhaustive high-vacuum dehydrated PM. Glucose-embedment concentration 0.25%.

the PM. All three perturbations of the PM cause a small decrease in the phenylalanine band at ~262 nm. Also, while vacuum dehydration and dry-glycerol impregnation cause a very small increase in the tryptophan band at ~283 nm, glucose embedment causes no changes at this wavelength.

Evidently, the effects of glucose on the far- and near-UV OCD are very similar to those of vacuum dehydration and dry-glycerol impregnation. However, there are important differences in the dynamics of the glucose effect and the dynamics of the other two perturbation effects. The effects of vacuum dehydration and dry-glycerol impregnation are completely reversible upon reexposing such perturbed films to ambient humidity (average 50% relative humidity). This reversal is extremely rapid (47). In the case of glucose embedment, the spectral effects are stable at ambient humidity. By definition, dehydration involves virtual absence of water. Both high-vacuum and glycerol (due to its hygroscopic property) act as dehydrants in the membrane by removing water molecules. Spectral effects appear only when critical removal of water molecules has been achieved (47). The actions of glucose on the state of the water in the membrane are most likely more complex. Because glucose substitutes for water in a manner as yet poorly understood, in a sense it may act as a quasidehydrant in the membrane. Three lines of evidence suggest this possibility. (*a*) The bR segments in the PM film remain untilted immediately after the evaporation of all the free water from the layering glucose solution and only tilt after the film is incubated at 90% relative humidity for some time. (*b*) High-vacuum evacuation of glucose-embedded films produces no additional effects than those produced by glucose alone. A similar result was observed with high-vacuum evacuation of glycerol-impregnated films (47). (*c*) A tertiary structural change of the protein, which exposes the protein core to an aqueous external environment in hydrated films, would be expected to dramatically alter the near-UV OCD, as was observed in the case of light-bleached PM (20). But in dehydrated and glucose-embedded films, no water would be available to enter the protein core and alter local molecular environments and disrupt interactions responsible for the near-UV OCD, so the near-UV OCD may remain relatively unaffected.

Visible OCD spectra

The comparative visible OCD spectra, which are attributable to the retinylidene $\pi - \pi^*$ (NV_1) transitions of the bR, for the native, vacuum-dehydrated, and glucose-embedded PM films are given in Fig. 4. As has previously been shown, vacuum dehydration results in a partial transformation of the ground photostate bR_{568} of the bR to a higher energy ground state, bR_{530}, as well as to other intermediate states at lower energy (47). Similar results were also observed with dry-glycerol–impregnated PM films. It is apparent that, while glucose embedding seems not to have any significant effect on the energy of the retinylidence transition of the bR, there is a narrowing of the CD band. This may be because the retinal is somewhat more constrained in the glucose-embedded film. However, it is also possible that the O_{640} intermediate of bR, the presence of which is sometimes evident in films at critical humidity levels, is not trapped in the glucose-embedded films, perhaps because the photocycle may not be able to progress to this state.

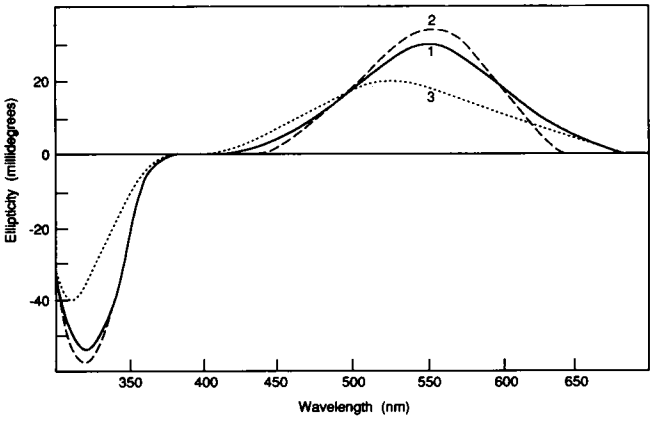

FIGURE 4 The film visible OCD spectra of (*1*) native, (*2*) glucose-embedded, and (*3*) exhaustive high-vacuum dehydrated PM. Glucose embedment concentration 0.25%.

It is obvious that, while glucose-embedded PM films demonstrate far- and near-UV spectral behavior similar to that of dehydrated PM films, their visible spectral behavior is notably different than those of the dehydrated films. One might argue that a tertiary structure change interpretation for the 23° $\Delta\theta_\alpha$ of glucose-embedded films is inconsistent with the apparent stability of the energy of the retinylidene transitions in such films. The energy of this transition has been suggested to be regulated by the average static asymmetric field imposed on the retinal by the apoprotein (59). Therefore, the most likely expectation would be that a tertiary structure change of the magnitude suggested by the $\Delta\theta_\alpha$ should be coupled to a significant change in this transition energy. However, does the absence of such changes unequivocally rule out the suggested tertiary structure change? If so, this would indeed present a serious paradox. But there is a way to avoid such a paradox. Consider the following facts. (*a*) In glucose-embedded PM films, no water is expected to be available to enter the protein core and alter significantly the average static field of the retinylidene environment. (*b*) The tilting of the bR segments away from the membrane normal may be occurring in such a manner to maintain the relative intersegmental parallelism (8). (*c*) Also, it has been observed that large changes in the retinylidene environment do not always result in changes in the transition energy. For example, the energy of retinylidene transition is nearly identical in PM in an aqueous or in a 80% glycerol environment. However, in the high-glycerol environment, both solution CD and film OCD suggested that either the sign of the average static asymmetric field or the screw sense imposed on retinal by the apoprotein had been reversed (49). In either case, this indicates significant structural alterations of the bR without any resulting changes in the retinylidene transition energy.

Conclusions

The stated purpose of glucose use in membrane studies is that glucose serves as an in vacuo preserver of biological structural integrity whenever high-vacuum dehydration is necessary (27, 28). It is generally assumed that sugars are a reasonable benign substitute for liquid water in membranes (1, 8, 27, 28, 30, 31, 43–46). Our efforts here are twofold: (*a*) to attempt to come to some consensus about the merits of this assumption about the benignity of glucose toward biological structures and (*b*) to attempt to bring to consolidation a number of conflicting findings published in the past about the structure and structural dynamics of bR in the PM.

Exhaustive dehydration of the PM results in a $\Delta\theta_\alpha$ of 22°, change in the retinylidene transition energy, and a disruption of the PM native crystalline order (28, 47). These changes can be interpreted as indicative of a major change in the orientation of the helical segments of bR (tertiary structure change), changes in the average static asymmetric field of the local protein environment of the retinal, and changes in the intermolecular interactions within the PM, which result in supramolecular structural changes in the PM. The fact that these changes result from the critical removal of liquid water from the membrane strongly suggests that liquid water is essential for maintaining the native structural integrity of the PM. Let us now compare the effects of glucose with the effects of dehydration on the structure of the PM. As demonstrated in the present studies, glucose embedding of the PM results in a very similar $\Delta\theta_\alpha$ and no change in the retinylidene transition energy. Also, it has been demonstrated in the past that a crystalline order is maintained in glucose-embedded PMs (8, 28). Clearly, the glucose effect seems in certain respects to be similar to the dehydration effect and dissimilar in other respects. Also, it has been shown that PMs perturbed either by dehydration or glucose embedding are capable of undergoing a photocycle of the bR, leading to the formation of a M_{412} intermediate (29, 60). Therefore, it can be concluded that the effects of the two perturbations on the nature of liquid water in the PM are not entirely similar. On the other hand, the effects of dry-glycerol impregnation are very similar to those of vacuum dehydration. Also, the effects of dry-glycerol and vacuum dehydration can be very rapidly completely reversed by reexposure to ambient humidity (average 50% relative humidity), while those of glucose remain stable under these conditions (47). Apparently glycerol acts as a dehydrant and removes liquid water as vacuum dehydration does. However, glucose does not act as a dehydrant in the same manner, but alters the nature of liquid water in the PM by substitution by a mechanism not yet clear. Further studies are necessary before a clear understanding of this mechanism can be achieved. Nevertheless, glucose seems to be an excellent substitute for the liquid water of the PM in regards to maintaining the supramolecular structure of the PM and also the average static field of the local protein environment of the retinal on the one hand, but a poor one, on the other hand, for maintaining the native orientations of the helical segments of the bR in the PM. On the basis of these observations, obviously, glucose cannot be considered to be entirely benign to PM structure.

Let us consider a number of conflicting findings concerning the native bR structure in the PM. Determinations of the θ_α of the native bR in the PM at ambient temperature by IRLD analysis have suggested this angle to be ~24–29° (22–26). However, these determinations were made on the assumption that the characteristics of the α-helices of the bR are exclusively of the α_I type. But there is very strong evidence (which has been summarized in the Introduction) that the amide planes of the α-helix of the bR are tilted on the average away from the helix axis by ~20–30° (10–19). Obviously, the IRLD determinations based on an α_I assumption are most likely not realistic and, therefore, such large θ_α values for the native bR in the PM should not be taken seriously.

On the other hand, if one considers the characteristics of the bR α-helices to be, on the average, ~60% α_I and 40% α_{II}, then a large number of experimental data could be brought into consistency. For example, the native state θ_α of the bR and the resulting $\Delta\theta_\alpha$ due to light bleaching of the bR of the PM in the presence of hydroxylamine are ~0 and 24°, respectively, when determined by the OCD and IRLD methods, but only when the IRLD analysis is based on a 60% α_I and 40% α_{II} assumption for the characteristics of the bR helices in the PM (17–19). Furthermore, a 60% α_I and 40% α_{II} characteristic for the α-helix of bR would provide a very reasonable explanation for the following observations. (*a*) The ellipticities of the CD band due to the n $-$ π^* transitions of the amides of the bR helix are relatively similar in magnitude in the OCD and solution spectra, when for an α_I helix they should be very different (12–15); (*b*) the ellipticities of the solution CD spectrum of bR are only two thirds of those of myoglobin over the entire far-UV wavelength range, in spite of the fact that these two proteins apparently have very similar α-helix content (12); (*c*) Raman spectroscopy detects only half of the helices of the bR being the α_I type (11); and (*d*) the amide I band behaves anomalously in the mid-IR spectrum of the bR (10).

If the θ_α for the native bR in the PM is ~0°, then the tilt of the helical segments of the bR away from the PM normal (resulting in a θ_α of ~11°) in the three-dimensional structural model of the bR of Henderson and coworkers (1, 8, 27–31), based on EMD studies, is most likely not a native characteristic of the bR but one induced by the glucose used in these studies. It seems logical to assume that if glucose can cause a $\Delta\theta_\alpha$ in PM films, it may also be able to do likewise in the glucose-embedded PM specimens used in EMD studies. The differences in magnitudes detected by the two methods may be due to the drastic differences in experimental conditions used by the two methods, especially temperature. Spectral studies were done at ambient temperature, while EMD studies were done at extremely low temperatures. It is expected that such low temperatures can restrict molecular dynamics and stabilize structure to some extent. However, there is data from two different sources that, it may be argued, contradicts this conclusion that the $\Delta\theta_\alpha$ of 11° detected by EMD studies is not a native characteristic of the native bR in the PM. (*a*) A comparative electron diffraction study of the PM prepared in glucose-embedded and ice-embedded states has been published (44). It was concluded that no major differences in PM structure are indicated by projected difference maps generated from the diffraction amplitudes of glucose-embedded minus ice-embedded specimens and the phases from published data for glucose-embedded specimens. The important point here is, Can one assume that the effects of water in the liquid state and the solid state are the same on the PM structure? Most likely, the effects of ice-embedding on the PM structure are more similar to those imposed by vacuum dehydrating, dry-glycerol impregnating, and glucose-embedding than those imposed by liquid water in the hydrous native state of the PM. A common feature of all these unnatural environments of the bR in the PM is that the nature of the water in membrane has been altered, in that the water molecule has either been removed or replaced or its state has been changed. This points out an important fact, that water in the liquid state is perhaps an essential factor of the native membrane structure. (*b*) Neutron- and x-ray–diffraction patterns of glucose-embedded PM specimens at low temperatures and wet and dried films at ambient temperature have all demonstrated fairly sharp and strong rings with basically similar intensity distributions, which are attributed to the periodic structure of the bR molecules packed in a p3 lattice (29, 33, 42). The analyses of neutron- and x-ray–diffraction data from hydrated PM have led to in-plane projected structures of the bR that are very similar to that suggested by EMD studies of glucose-embedded PM, particularly in agreement with helical segmental tilting. The only explanation that can be given for this seeming paradox at this time is that diffraction analyses, which are based on a structure modeling and statistical data-fitting computational methodology, are comparatively rather limited in resolution power. Therefore, small structural differences could be masked by the differences in the inherent resolution powers of the various techniques used.

Let us now consider the conflicting findings concerning the photoinduced structural dynamics of the bR in the PM. OCD studies of hydrated PM films have detected a $\Delta\theta_\alpha$ of 10 ± 5° at −70°C resulting from the transformation of the ground state, bR_{568}, to the excited photointermediate state, M_{412}, of the bR (34). However, EMD studies using glucose-embedded PM specimens did not detect any changes (29). Recently, a number of studies of glucose-free PM specimens using Fourier transform IR, neutron, and x-ray diffraction methods have detected changes of various magnitudes, depending on the experimental conditions used (38–42). It seems that glucose embedding may be the key factor for these conflicting findings about structural changes due to this state transformation of the bR. Glucose is somehow preventing these changes observed in glucose-free PM. Surprisingly, a number of diverse perturbations of the PMs result in a very similar $\Delta\theta_\alpha$ value of 22 ± 2° at ambient temperature (17, 18, 47, 55). In addition, a combination of two perturbing factors does not seem to affect this apparently limiting value of $\Delta\theta_\alpha$. However, when the PM is chemically altered by a variety of different agents, θ_α remains unchanged from the native value of ~0° (18). But when these PMs are subjected to light bleaching, at ambient temperatures, the resulting $\Delta\theta_\alpha$ is not 22 ± 2°, as in the native case, but an enhanced 36 ± 2.5°. One explanation for these results may be that there is an inherent instability in the native bR structure in the PM that regulates the magnitude of $\Delta\theta_\alpha$ when the PM is perturbed

to a limiting value. So far, this limit seems to be essentially independent of the perturbing factor used. Chemical alteration of the PM results in enhancement of this native instability, leading to a higher $\Delta\theta_\alpha$ value. It is expected that the limiting $\Delta\theta_\alpha$ value of native bR would be lower at very low temperatures since low temperatures may be able to reduce the hypothetical structural instability of native bR. Therefore, it is possible that the limiting $\Delta\theta_\alpha$ value could be $\sim 10 \pm 5°$ at low temperatures. Since glucose-embedded specimens are used in the EMD studies of the bR_{568}-to-M_{412} transformation at very low temperatures, this would result in a combination of two perturbing factors. If the first factor, glucose, has resulted in this low-temperature limiting value of $\Delta\theta_\alpha$'s being reached, further changes due to a second factor, state transformation, may not be observed because of the masking effects of the first.

It is clear that a consistent explanation is possible that can bring all these conflicting findings of the structure and the dynamics of the bR in the PM from past studies into agreement. However, this can be accomplished only if one considers two experimentally well-supported findings concerning the in situ structure and dynamics of the bR in the PM. (a) The structural characteristics of the α-helices of the bR are very different from those usually given for extrinsic proteins in current literature. (b) The bR is inherently capable of dramatic reversible structural dynamics in response to the actions of a number of diversified perturbations of the PM.

Received for publication 23 December 1991 and in final form 28 December 1992.

REFERENCES

1. Henderson, R. 1977. The purple membrane from *Halobacterium halobium*. *Annu. Rev. Biophys. Bioeng.* 6:87–109.
2. Eisenbach, M., and S. R. Caplan. 1979. The light-driven pump of *Halobacterium halobium*: mechanism and function. *Curr. Top. Membr. Transp.* 12:165–248.
3. Stoeckenius, W., R. H. Lozier, and R. A. Bogomolni. 1979. Bacteriohodopsin and the purple membrane of halobacteria. *Biochim. Biophys. Acta.* 505:215–278.
4. Ottolenghi, M. 1980. The photochemistry of rhodopsin. *Adv. Photochem.* 12:97–200.
5. Stoeckenius, W., R. H. Lozier, and R. A. Bogomolni. 1981. Bacteriorhodopsin photocycle and stoichiometry. *In* Chemisosmotic Proton Circuits in Biological Membranes. V. P. Skulachev and P. C. Hinkle, editors. Wesley Publishing Co., Inc., Reading, MA. 283–309.
6. Stoeckenius, W., and R. A. Bogomolni. 1982. Bacteriorhodopsin and related pigments of halobacteria. *Annu. Rev. Biochem.* 51:587–616.
7. Dencher, N. A. 1983. The five retinal protein pigments of halobacteria: bacteriorhodopsin, halorhodopsin, P565, P370 and slow-cycling rhodopsin. *Photochem. Photobiol.* 37:753–767.
8. Henderson, R., J. M. Baldwin, T. A. Ceska, F. Zemlin, E. Beckmann, and K. H. Downing. 1990. Model for the structure of bacteriorhodopsin based on high-resolution electron cryo-microscopy. *J. Mol. Biol.* 213:899–929.
9. Némethy, G., D. C. Phillips, S. J. Leach, and H. A. Scheraga. 1967. A second right-handed helical structure with parameters of the Pauling-Corey α-helix. *Nature (Lond.).* 214:363–365.
10. Krimm, S., and A. M. Dwivedi. 1982. Infrared spectrum of the purple membrane: clue to a proton conduction mechanism? *Science (Wash. DC).* 216:407–408.
11. Vogel, H., and W. Gärtner. 1987. The secondary structure of bacteriorhodopsin determined by Raman and circular dichroism spectroscopy. *J. Biol. Chem.* 262:11464–11469.
12. Gibson, N. J., and J. Y. Cassim. 1989. Evidence for an α_{II}-type helical conformation for bacteriorhodopsin in the purple membrane. *Biochemistry.* 28:2134–2139.
13. Schellman, J. A. and R. Oriel. 1962. Origin of the Cotton effect of helical polypeptides. *J. Chem. Phys.* 32:2114–2120.
14. Woody, R. W., and I. Tinoco, Jr. 1967. Optical rotation of oriented helices. III. Calculations of the rotatory dispersion and circular dichroism of the alpha and 3_{10}-helix. *J. Chem. Phys.* 46:4927–4945.
15. Hofrichter, H. J. 1971. A general phase modulation spectrophotometer: studies on shear oriented biopolymers. Ph.D. thesis. The University of Oregon, Eugene, Oregon. 286 pp.
16. Olah, G. A., and H. W. Huang. 1988. Circular dichroism of oriented α helices. I. Proof of the exciton theory. *J. Chem. Phys.* 89:2531–2538.
17. Draheim, J. E., N. J. Gibson, and J. Y. Cassim. 1991. Dramatic *in situ* conformational dynamics of the transmembrane protein bacteriorhodopsin. *Biophys. J.* 60:89–100.
18. Gibson, N. J., and J. Y. Cassim. 1989. Nature of forces stabilizing the transmembrane protein bacteriorhodopsin in purple membrane. *Biophys. J.* 56:769–780.
19. Draheim, J. E., and J. Y. Cassim. 1992. % alpha-II helix in bacteriorhodopsin. *Biophys. J.* 61:552*a*. (Abstr.)
20. Muccio, D. D., and J. Y. Cassim. 1979. Interpretation of the absorption and circular dichroism spectra of oriented purple membrane films. *Biophys. J.* 26:427–440.
21. Wu, Y., H. W. Huang, and G. A. Olah. 1990. Method of oriented circular dichroism. *Biophys. J.* 57:797–806.
22. Rothschild, K. J., and N. Clark. 1979. Polarized infrared spectroscopy of oriented purple membrane. *Biophys. J.* 25:473–488.
23. Aldashev, A. A. 1985. Orientations of α-helix rods in bacteriorhodopsin and bacterioopsin. *Biol. Membr.* 2:363–366.
24. Nabedryk, E., A. M. Bardin, and J. Breton. 1985. Further characterization of the protein secondary structure in purple membrane by circular dichroism and polarized infrared spectroscopies. *Biophys. J.* 48:873–876.
25. Earnest, T. N. 1987. Fourier transform infrared and resonance Raman spectroscopic studies of bacteriorhodopsin. Ph.D. dissertation. Boston University, Boston, MA. 193 pp.
26. Earnest, T. N., J. Herzfeld, and K. J. Rothschild. 1990. Polarized fourier transform infrared spectroscopy of bacteriorhodopsin: transmembrane alpha helices are resistant to hydrogen/deuterium exchange. *Biophys. J.* 58:1539–1546.
27. Henderson, R., and P. N. T. Unwin. 1975. Three-dimensional model of purple membrane obtained by electron microscopy. *Nature (Lond.).* 257:28–32.
28. Unwin, P. N. T., and R. Henderson. 1975. Molecular structure determination by electron microscopy of unstained crystalline specimens. *J. Mol. Biol.* 94:425–440.
29. Glaeser, R. M., J. M. Baldwin, T. A. Ceska, and R. Henderson. 1986. Electron diffraction analysis of the M_{412} intermediate of bacteriorhodopsin. *Biophys. J.* 50:913–920.
30. Henderson, R., J. M. Baldwin, K. H. Downing, J. Lepault, and F. Zemlin. 1986. Structure of purple membrane from *Halobacterium halobium*: recording, measurement and evaluation of elec-

tron micrographs at 3.5 Å resolution. *Ultramicroscopy.* 19:147–178.

31. Baldwin, J. M., R. Henderson, E. Beckmann, and F. Zemlin. 1988. Images of purple membrane at 2.8 Å resolution obtained by cryo-electron microscopy. *J. Mol. Biol.* 202:585–591.
32. Nabedryk, E., and J. Breton. 1981. Orientation of intrinsic proteins in photosynthetic membranes: polarized infrared spectroscopy of chloroplasts and chromatophores. *Biochim. Biophys. Acta.* 635:515–524.
33. Henderson, R. 1975. The structure of the purple membrane from *Halobacterium halobium:* analysis of the x-ray diffraction pattern. *J. Mol. Biol.* 93:123–138.
34. Draheim, J. E., and J. Y. Cassim. 1985. Large scale global structural changes of the purple membrane during the photocycle. *Biophys. J.* 47:497–507.
35. Bagley, K., G. Dollinger, L. Eisenstein, A. K. Singh, and L. Zimányi. 1982. Fourier transform infrared difference spectroscopy of bacteriorhodopsin and its photoproducts. *Proc. Natl. Acad. Sci. USA.* 79:4972–4976.
36. Earnest, T. N., P. Roepe, M. S. Braiman, J. Gillespie, and K. J. Rothschild. 1986. Orientation of the bacteriorhodopsin chromophore probed by polarized fourier transform infrared difference spectroscopy. *Biochemistry.* 25:7793–7798.
37. Nabedryk, E., and J. Breton. 1986. Polarized fourier transform infrared (FTIR) difference spectroscopy of the M_{412} intermediate of bacteriorhodopsin. *FEBS (Fed. Eur. Biochem. Soc.) Lett.* 202:356–360.
38. Braiman, M. S., P. L. Ahl, and K. J. Rothschild. 1987. Millisecond FTIR-transform infrared difference spectra of bacteriorhodopsin's M_{412} photoproduct. *Proc. Natl. Acad. Sci. USA.* 84:5221–5225.
39. Ormos, P. 1991. Infrared spectroscopic demonstration of a conformational change in bacteriorhodopsin involved in proton pumping. *Proc. Natl. Acad. Sci. USA.* 88:473–477.
40. Dencher, N. A., D. Dresselhaus, G. Zaccai, and G. Büldt. 1989. Structural changes in bacteriorhodopsin during proton translocation revealed by neutron diffraction. *Proc. Natl. Acad. Sci. USA.* 86:7876–7879.
41. Nakasko, M., M. Kataoka, Y. Amemiya, and F. Tokunaga. 1991. Crystallographic characterization by x-ray diffraction of the M-intermediate from the photo-cycle of bacteriorhodopsin at room temperature. *FEBS (Fed. Eur. Biochem. Soc.) Lett.* 292:73–75.
42. G. Büldt, N. A. Dencher, H. J. Plöhn, D. Oesterhelt, G. Rapp, and M. H. J. Koch. 1992. Time-resolved x-ray diffraction and neutron scattering study of structure changes associated with the photocycle of bacteriorhodopsin. *Abstracts of the Vth International Conference on Retinal Proteins, June 28–July 3, 1992, Dourdan, France.*
43. Hayward, S. B., and R. M. Stroud. 1981. Projected structure of purple membrane determined to 3.7 Å resolution by low temperature electron microscopy. *J. Mol. Biol.* 151:491–517.
44. Jaffe, J. S., and R. M. Glaeser. 1987. Difference Fourier analysis of "surface features" of bacteriorhodopsin using glucose-embedded and frozen-hydrated purple membrane. *Ultramicroscopy.* 23:17–28.
45. Mitra, A. K., and R. M. Stroud. 1990. High sensitivity electron diffraction analysis: a study of divalent cation binding to purple membrane. *Biophys. J.* 57:301–311.
46. Sikerwar, S. S., K. H. Downing, and R. M. Glaeser. 1991. Three-dimensional structure of an invertebrate innercellular communicating junction. *J. Struct. Biol.* 106:255–263.
47. Draheim, J. E., N. J. Gibson, and J. Y. Cassim. 1988. Dehydration-induced structural changes of purple membrane of *Halobacterium halobium. Biophys. J.* 54:931–944.
48. Becher, B., and J. Y. Cassim. 1975. Improved isolation procedures for the purple membrane of *Halobacterium halobium. Prep. Biochem.* 5:161–178.
49. Draheim, J. E., and J. Y. Cassim. 1985. Effects of polyhydric alcohols on the conformational stability of the purple membrane. *J. Membr. Biol.* 86:229–238.
50. Fisher, K. A. 1982. Preparation of planar membrane monolayers for spectroscopy and electron microscopy. *Methods Enzymol.* 88:230–235.
51. Heyn, M. P., R. J. Cherry, and U. Müller. 1977. Transient and linear dichroism studies on bacteriorhodopsin: determination of orientation of the 568 nm all-*trans* retinal chromophore. *J. Mol. Biol.* 117:607–620.
52. Woody, R. W. 1985. Circular dichroism of peptides. *Peptides (NY).* 7:15–114.
53. Urry, R. W., and M. M. Long. 1978. Ultraviolet absorption, circular dichroism, and optical rotatory dispersion in biomembrane studies. *In* Physiology of Membrane Disorder. T. E. Andreoli, J. F. Hoffman, and D. D. Fanestil, editors. Plenum Medical Book Co., New York. 107–124.
54. Gibson, N. J. 1988. An analysis of the secondary and tertiary structure of the membrane protein bacteriorhodopsin and changes induced by glucose or reduction of the retinal-lysine linkage. Ph.D. thesis. The Ohio State University, Columbus, OH. 258 pp.
55. Cassim, J. Y., J. E. Draheim, and N. J. Gibson. 1992. The *in situ* molecular dynamics of the transmembrane protein bacteriorhodopsin: static or kinetic? *In* Structures and Functions of Retinal Proteins. J. L. Rigaud, editor. Colloque Inserm/John Libbey Eurotext Ltd. Vol. 221, Montrouge, France. 25–28.
56. Bazzi, M. D., and R. W. Woody. 1985. Oriented secondary structure in integral membrane proteins. *Biophys. J.* 48:957–966.
57. Glaeser, R. M., K. H. Downing, and B. K. Jap. 1991. What spectroscopy can still tell us about the secondary structure of bacteriorhodopsin. *Biophys. J.* 59:934–938.
58. Engleman, D. M., and G. Zacci. 1980. Bacteriorhodopsin is an inside-out protein. *Proc. Natl. Acad. Sci. USA.* 77:5894–5898.
59. Honig, B., and T. Ebrey. 1974. The structure and spectra of the chromophore of visual pigments. *Annu. Rev. Biophys. Bioeng.* 3:151–177.
60. Hildebrandt, P., and M. Stockburger. 1984. Role of water in bacteriorhodopsin's chromophore: resonance Raman study. *Biochemistry.* 23:5539–5548.